Segmental and Chain Dynamics of Polyisoprene in Block Copolymer/ Homopolymer Blends. A Dielectric Spectroscopy Study

G. Floudas* and K. Meramveliotaki

Foundation for Research and Technology- Hellas (FORTH), Institute of Electronic Structure and Laser, P.O. Box 1527, 711 10 Heraklion Crete, Greece

N. Hadjichristidis

Department of Chemistry, University of Athens, Zografou 15771 Athens, Greece, and Foundation for Research and Technology- Hellas (FORTH), Institute of Electronic Structure and Laser, P.O. Box 1527, 711 10 Heraklion Crete, Greece

Received April 8, 1999; Revised Manuscript Received August 26, 1999

ABSTRACT: The local and global dynamics of polyisoprene (PI) have been studied in a well-defined restricted environment. The restriction is provided by the thermodynamic field of segregated poly(styrene-*b*-isoprene) (SI) diblock copolymers. The copolymers were nearly symmetric in composition, and the amount of added PI's was kept below 20% to ensure the absence of macrophase separation in the blends. Two studies have been made. In the first study, different PI's with molecular weights in the range from 1.2 $\times$ 10^3 to 5.5 $\times$ 10^4 have been added to a symmetric SI diblock copolymer. We found that both the homopolymer and PI block dynamics are modified in the blends, and the degree of modification can be qualitatively accounted for by the reptation and arm-retraction mechanisms, respectively. A quantitative comparison, however, would require an unrealistic increase of the entanglement molecular weight. In addition, for the higher molecular weight homopolymers there is an effect on the homopolymer chain dynamics due to the confinement within the center of the lamellae. In a second study, the same PI was inserted in different (symmetric) SI diblock copolymers with an increasing degree of segregation. We found a dynamic signature of the homopolymer localization imposed by the thermodynamic field. Block copolymer/homopolymer blends are model systems for studying the effect of confinement on the local and global dynamics.

I. Introduction

Recently there has been an increasing effort to understand, control, and ultimately predict the properties of liquids near surfaces and interfaces and within porous media. These efforts are likely to have, apart from fundamental, also technological importance in fields such as membrane separation, chromatography, and oil recovery. There is consensus that both the static and the dynamic properties of liquids are altered in the vicinity of an interface. For example, the melting temperature of liquids immersed in porous glasses is strongly suppressed,[1] and the glass transition temperature is also affected as a result of the confinement.[2,3] Recently we have shown[4] that the chain relaxation of polyisoprene (PI) is also affected by the confinement within the controlled porous glass (CPG) Bioran. One disadvantage of the porous glasses used for the majority of the studies of liquid confinement is that they exhibit a broad pore-size distribution, and in many cases the pores have very irregular shapes. Therefore, these systems cannot be considered as model systems.

A way to overcome this difficulty is by new synthetic roots of inorganic materials with well-controlled sizes. Another way is by investigating polymer dynamics within the restricted geometries formed by microphase separated block copolymers. It is the latter system which is of interest to us here. It has been predicted theoretically[5] and verified experimentally[6] that the dissimilarity of the two blocks in an AB diblock copolymer drives the system from a homogeneous disordered state, at small values of the product χN (where χ is the segment−segment interaction parameter, which in the simplest approximation is inversely proportional to temperature, and N is the total degree of polymerization), to spatially heterogeneous microdomains composed from A and B blocks. This microphase separation occurs for χN values of 10.5 for the symmetric case ($f = 0.5$, where f is the volume fraction of the A blocks). The geometry (spheres, cylinders, lamellae) and size (5−500 nm) of the microdomains can be controlled at the synthesis level. This observation brings forward a new possibility of studying the effect of restriction on the polymer dynamics. The only difference from other porous systems based on inorganic materials is that the confinement is provided here by the same chains that make up the domains.

Herein we study the effect of confinement of various homopolymers immersed within the microdomains of diblock copolymers. The distribution of added homopolymer within the domains depends on the block and homopolymer molecular weights and is determined by two opposing factors; the blocks expel the homopolymer toward the lamellar center, but entropic factors favor a uniform density and thus a more uniform distribution of the homopolymer. The thermodynamic field and the topological constraints are expected to alter the homopolymer dynamics in comparison to the bulk.

For our investigation we chose the poly(styrene-*b*-isoprene) (SI) diblock copolymer system and added homo-polyisoprenes of carefully chosen molecular weights. The range of molecular weights and composition was such that no macrophase separation took place.[7] Polyisoprene (cis-PI) is a type A polymer with components of the dipole moment both perpendicular and parallel to the chain, giving rise to local segmental and chain relaxations, respectively.[8] The technique is dielectric spectroscopy (DS) which is very sensitive to the dipolar relaxations and has the required broad frequency range to capture the multiple relaxation

10.1021/ma990524n CCC: $18.00
Published on Web 10/12/1999

Table 1. Molecular Characteristics of the Polyisoprenes (PI)

sample	$10^{-3}M_n$[a]	$10^{-3}M_w$[b]	M_w/M_n[c]
PI-1200	1.2[d]	1.3	1.10
PI-2500	2.5[d]	2.6	1.05
PI-4900	4.9[d]	5.2	1.05
PI-6800	6.5[e]	6.9[e]	1.07[e]
PI-10500	10.5[e]	10.8[e]	1.03[e]
PI-20500	20.5	21.5	1.05
PI-45200	45.2	47.5	1.05
PI-55000	55.0	57.8	1.05
PI-90000	90.0	93.6	1.04

[a] Membrane osmometry in toluene at 35 °C. [b] Low angle laser light scattering in cyclohexane at 25 °C. [c] Size exclusion chromatography in THF at 30 °C. [d] Vapor pressure osmometry in toluene at 50 °C. [e] Samples and values provided by PSS, Mainz, Germany.

Table 2. Molecular Characteristics of the Poly(styrene-*b*-isoprene) (SI) Block Copolymers

sample	$10^{-3}M_n$[a]	M_w/M_n[b]	w_{PS}[c] (%)	f_{PS}[d]	χN
SI-15200	15.2	1.04	0.50	0.46	16.3
SI-22500	22.5	1.04	0.55	0.51	21
SI-31000	31.6	1.03	0.54	0.5	25
SI-41000	40.5	1.04	0.52	0.48	28

[a] Membrane osmometry in toluene at 30 °C. [b] Size exclusion chromatography in THF at 30 °C. [c] ^{1}H NMR in $CDCl_3$ at 30 °C. [d] Calculated from $N_n = N_{n,PS}^* + N_{n,PI}^* = N_{n,PS}\sqrt{(\rho_I^*/\rho_S^*)} + N_{n,PI}\sqrt{(\rho_S^*/\rho_I^*)}$ and $f_{PS} = N_{n,PS}^*/N_n$ where $N_{n,i}$ are the degrees of polymerization of each block and ρ_i^* are the molar densities.

processes. In a recent study[9] we were able to probe the interface of linear[9c] and nonlinear[9b] block copolymers with a basic triblock unit. In another study[9d] we were able to identify the relevant topological effects on the dynamics of ordered star block copolymers. Given the success of DS in identifying the local and global dynamics in topologically complex block copolymers, we continue employing this method to investigate the interplay between structure and dynamics in the SI/PI blends.

II. Experimental Section

Materials. The poly(styrene-*b*-isoprene) (SI) and polyisoprene-1,4 (PI) samples were synthesized by anionic polymerization (*sec*-BuLi, benzene, room temperature) using high-vacuum techniques. The molecular characteristics of the PI homopolymer and SI diblock copolymer samples are given in Tables 1 and 2, respectively.

Differential Scanning Calorimetry (DSC). A Polymer-Laboratories DSC was used with an integral cooling jacket capable of programmed cyclic temperature tests over the range −160 to 400 °C. A dry gas purge was used for accurate measurements near ambient temperature ranges. Two cooling and heating cycles have been performed (with a rate of 10 K/min), and the results of the second heating run for the glass transition temperatures (T_g) and widths (ΔT_g) are depicted in Table 3.

Small-Angle X-ray Scattering (SAXS). A Kratky compact camera (Anton Paar KG) equipped with a one-dimensional position-sensitive detector (M. Braun) was used for the SAXS experiment. The Ni-filtered Cu Kα radiation ($\lambda = 0.154$ nm) was used from a Siemens generator operating at 35 kV and 30 mA. Measurements of 1 h long were made at intervals of 5 K within the range 303−423 K, and the stability was better than ±0.2 K. Changes between successive temperatures were completed within ∼5 min, and a 30 min waiting time was preset for equilibration. The smeared intensity data were collected in a multichannel analyzer and transferred to a PC for further analysis. Smeared intensities were subsequently corrected for absorption, background scattering and slit-length smearing. Primary beam intensities were determined, in absolute units, by using the moving slit method. Some typical

Table 3. DSC Glass Transition Temperatures (Heating Rate 10 K/min) and Breadth (ΔT_g) for the Homopolymer, Diblock Copolymers, and Their Blends

sample	T_g^{PI} (ΔT_g) (K)	T_g^{PS} (ΔT_g) (K)
PI-1200	193 (8)	
PI-2500	199 (9)	
PI-4900	204 (8)	
PI-20500	206 (8)	
PI-45200	206 (8)	
PI-55000	206 (8)	
SI-22500	206 (8)	333 (52)
SI-31000	206 (8)	339 (56)
SI-41000	206 (8)	341 (54)
SI-22500/PI-1200 (80/20)	200 (8)	328 (45)
SI-22500/ PI-4900 (80/20)	203 (8)	334 (44)
SI-22500/ PI-20500 (80/20)	205 (7)	334 (40)
SI-22500/ PI-45000 (80/20)	205 (7)	334 (41)
SI-22500/ PI-55000 (80/20)	205 (8)	333 (48)

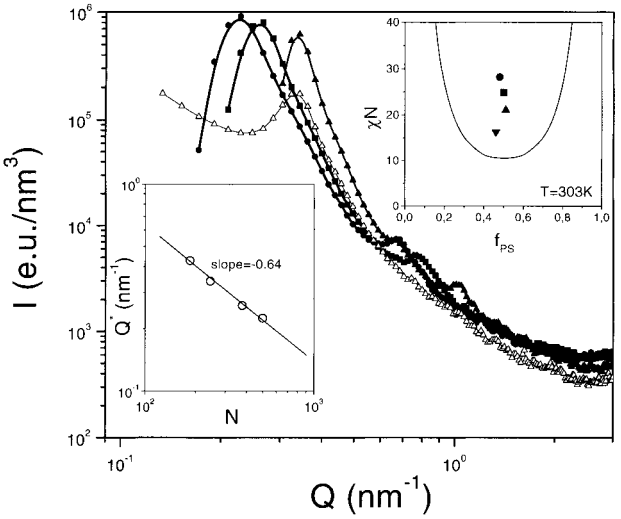

Figure 1. SAXS spectra of three SI diblock copolymers (triangles, SI-22500; squares, SI-31000; circles, SI-41000) and a blend SI-22500/PI-1200 (80/20) (open triangles) taken at 303 K. In the lower inset we plot the peak position (Q^*) as a function of the total degree of polymerization N for the four nearly symmetric diblock copolymers investigated. The slope is −0.64. In the upper inset we position the four diblock copolymers within the mean-field phase diagram.

SAXS spectra are shown in Figure 1 for three of the diblock copolymers and one of the blends.

Dielectric Spectroscopy (DS). Measurements of the complex dielectric function have been made with a Novocontrol BDC-S system composed of a frequency response analyzer (Solartron Schlumberger FRA 1260) and a broad-band dielectric converter with an active sample cell. The latter contains six reference capacitors in the range from 25 to 1000 pF. Measurements were made in the frequency range from 10^{-2} to 10^6 Hz using a combination of three capacitors in the active sample cell. The resolution in tand was about 2×10^{-4} in the frequency range between 10^{-1} and 10^5 Hz. The samples were kept between two gold-plated stainless steel plates of 20 mm diameter with a separation of 100 μm which resulted in a sample capacitance of about 100 pF. Care was taken so that the samples completely filled the capacitor cell. The sample cell was set in the cryostat, and the sample temperature was controlled between 213 and 413 K and measured with a PT100 sensor in the lower plate of the sample capacitor with an accuracy of ±0.05 K. Some typical dielectric loss curves for the SI-22500/PI-1200 blend are shown in Figure 2.

III. Data Analysis

The complex dielectric permittivity, $\epsilon^*(\omega) = \epsilon'(\omega) - i\epsilon''(\omega)$ of a macroscopic system is given by the Fourier−Laplace transform of the time derivative of the normal-

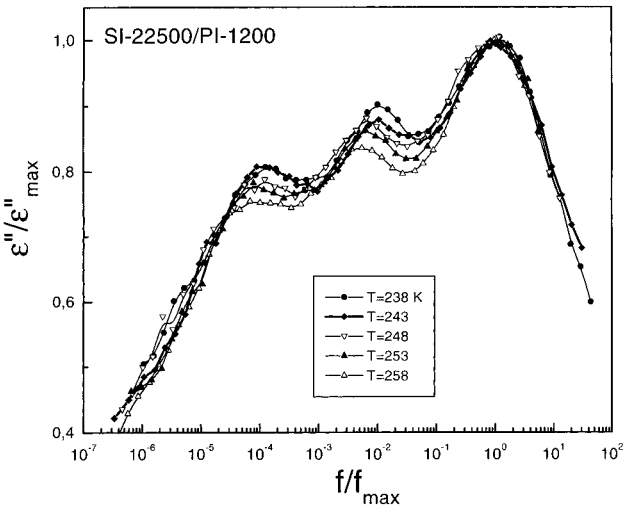

Figure 2. Representative dielectric loss spectra of the SI-22500/PI-1200 (80/20) blend shown for different temperatures as indicated. Three processes are shown: a "fast" segmental mode, an intermediate mode corresponding to the normal mode of PI-1200 in the blend, and a "slow" mode due to the PI block relaxation. The axes have been normalized to the fast segmental peak revealing that the two slow modes start to approach to the segmental mode with decreasing temperature (see text).

ized response function $\Phi(t)$ of the polarization $\mathbf{P}(t)$ of the system:

$$\frac{\epsilon^*(\omega) - \epsilon_\infty}{\Delta\epsilon} = \int_0^\infty e^{-i\omega t}\left(-\frac{d\Phi}{dt}\right) dt \qquad (1)$$

where ϵ_0 and ϵ_∞ are the limiting low- and high-frequency permittivities, respectively, and $\Delta\epsilon$ ($= \epsilon_0 - \epsilon_\infty$) is the relaxation strength. $\Phi(t)$ is given by

$$\Phi(t) = \frac{\langle P(t)\cdot P(0)\rangle}{\langle P(0)\cdot P(0)\rangle} \qquad (2)$$

In eq 2 the polarization $\mathbf{P}(t)$ is given by the sum of all dipoles in the system. $\Phi(t)$ can be decomposed into two components: one related to dipole moments parallel $\mu^{\parallel}$ to the chain contour and another to dipole moments perpendicular $\mu^{\perp}$ to the chain contour. The two components give rise to the global normal mode and the local segmental relaxation processes, respectively. In principle, $\mathbf{P}(t)$ contains intra- and intermolecular contributions. However, measurements of the dielectric strength as a function of polymer concentration in solutions of cis-PI in the Θ solvent dioxane up to the bulk revealed that intermolecular dipole−dipole interactions are negligible.[8c] Furthermore, ignoring the cross terms between the parallel and perpendicular components, we can write for the parallel component in $\Phi(t)$ which correspond to the end-to-end vector motion:

$$\sum_j \sum_m \langle \mu_{ij}''(0)\cdot\mu_{im}''(t)\rangle = \mu^2\langle r_i(0)\cdot r_i(t)\rangle \qquad (3)$$

where μ is the dipole moment per contour length. Since the relaxation times of the two components present in $\Phi(t)$ are well separated in the time domain, the individual autocorrelation functions can be calculated. Thus, the complex dielectric constant due to the normal mode process is given by the Fourier−Laplace transform of the autocorrelation function $\langle \mathbf{r}(0)\cdot\mathbf{r}(t)\rangle/\langle r^2\rangle$ for the end-to-end vector:

$$\frac{\epsilon^*(\omega) - \epsilon_\infty}{\Delta\epsilon} = \frac{1}{\langle r^2\rangle}\int_0^\infty e^{-i\omega t}\left[-\frac{d\langle r(0)\cdot r(t)\rangle}{dt}\right] dt \qquad (4)$$

where $\langle r^2\rangle$ denotes the mean-square end-to-end distance and $\Delta\epsilon$ ($= \epsilon_0 - \epsilon_{\infty,n}$) is the relaxation strength for the normal mode process with $\Delta\epsilon_{\infty,n}$ being the high-frequency limit of the process under investigation.

To analyze the isothermal spectra of the dielectric loss ϵ'', we have used the empirical function of Havriliak and Negami (HN):

$$\frac{\epsilon^*(\omega) - \epsilon_\infty}{\Delta\epsilon} = \frac{1}{[1 + (i\omega\tau_{HN})^\alpha]^\gamma} \qquad (5)$$

where τ_{HN} is the characteristic relaxation time. The parameters α and γ describe respectively the symmetrical and asymmetrical broadening of the distribution of relaxation times. In a log ϵ'' vs log ω plot, α and $\alpha\gamma$ give respectively the low- and high-frequency slopes of the relaxation function. The fitting procedure was as follows: For the PI homopolymers two HN functions were used to represent the fast segmental ($\alpha_s = 0.6$, $\gamma_s = 0.7$) and slow normal modes ($\alpha_n = 1$), and the τ_{max} was obtained for both modes. Here we should mention that a single HN cannot capture the full dielectric loss spectra for the normal modes especially for the higher molecular weights. The analysis of the full normal mode spectrum of polyisoprenes will be reported elsewhere.[10] Here we refer to the longest normal mode which well corresponds to the maximum loss. For the blends with $0.3N_{PI,block} < N_h < 3N_{PI,block}$ two HN functions were used to describe the segmental mode (with fixed shape parameters to the homopolymer case) and single normal mode. For the blends with N_h outside this range we have used three HN functions to describe the single segmental mode and the two chain modes corresponding to the block and homopolymer relaxations. Because of the large number of parameters involved, we have fixed the shape parameters for the segmental mode and the homopolymer normal mode to the bulk PI values. The errors in the four parameters $\Delta\epsilon$, α, γ, and τ describing the "slow" chain mode were 10, 7, 8, and 8%, respectively.

IV. Results and Discussion

Structure. Prior to the dielectric investigation of the homopolymer dynamics in the restricted environment of the microdomains, we have explored the phase state of the block copolymers and their blends with different PI homopolymers. Recently we have investigated block copolymer/homopolymer blends with respect to the order-to-disorder transition temperature.[7] We found that a small amount of a homopolymer can control the compatibility between the two blocks. Moreover, keeping the concentration of added homopolymer to below 20% resulted in a single microdomain structure; i.e., no macrophase separation takes place. In the present study we kept the PI homopolymer concentration to below 20%, which guarantees that the homopolymer is located within the SI microdomains. Figure 1 gives the SAXS spectra for three of the symmetric diblock copolymers and one blend (SI-41000/PI-1200). The high peak intensity $I(Q^*)$ and the existence of a higher order peak at position $3Q^*$ signifies the formation of lamellae with approximately equal domain sizes for the PI and PS domains. The peak position at Q^* shifts with the total

degree of polymerization N (shown in the lower inset to Figure 1) as $Q^* \sim N^{-0.64}$ due to the increasing degree of segregation. The position of the four diblock copolymers in the mean-field phase diagram is shown in the upper inset to Figure 1. For the χ parameter we have used ref 11. The χN values are in the range 16−28, that is, in some intermediate range between the weak segregation limit ($10.5 < \chi N < 12.5$, with a scaling for the long spacing D ($=2\pi/Q^*$) as $N^{1/2}$) and the strong segregation limit (SSL) ($\chi N > 100$, with $D \sim N^{2/3}$).[12] For this intermediate segregation regime recent density functional theory[13] predicts $D \sim N^{0.72}$, which is a slightly steeper N dependence. Our data shown in the inset have a slope of 0.64, in accord with the prediction from the SSL; however, the range of molecular weights is small, and a slightly steeper N dependence as predicted by the theory cannot be totally excluded.

In the blends, we found that there is a small increase of the long spacing. However, the lamellar spacing is not the appropriate quantity to discuss morphological changes in block copolymer/homopolymer blends, since it does not account for the separate (and opposing) effects of the layer thicknesses.[14,15] For this reason we are using the overall PS volume fraction ($f_{PS}' = f_{PS}(1 - \varphi_{PI})$, where φ_{PI} is the concentration of the added PI homopolymer) and calculate the overall PI and PS layer thicknesses and the average area per junction at the interface:

$$l_{PS} = f_{PS}'D$$

$$l_{PI} = f_{PI}'D$$

$$\sigma = \frac{2M_{PS}}{N_A \rho_{PS} l_{PS}} \qquad (6)$$

where M_{PS} is the PS block molecular weight and ρ_{PS} ($\approx$1.05 g/cm^3) is the PS density. The layer thicknesses and the area per junction provide the morphological changes in the axial and lateral directions, respectively. We found that addition of PI has opposite results on the PS and PI layer thicknesses which have been found to decrease and increase, respectively. Furthermore, σ was found to increase with homopolymer addition. For example, the pure diblock SI-22500 values are $l_{PS} = 9.44$ nm, $l_{PI} = 9.1$ nm, and $\sigma = 41.4$ nm^2. In the SI-22500/PI-2500 (80/20) blend the corresponding values are $l_{PS} = 7.4$ nm, $l_{PI} = 10.5$ nm, and $\sigma = 53.2$ nm^2. Therefore, although there are minor effects on the long period, there is an axial contraction on the PS layer and an axial expansion on the PI layer which are accompanied by lateral expansion of the junction points at the interface. For higher molecular weights the lateral expansion deminishes, signifying that the morphological changes are a function of the homopolymer length.

The localization of the homopolymer is determined by two opposing factors:[15] the blocks tend to expel the homopolymer away from the junction points toward the lamellar center, but this action is countered by the entropy of mixing which tends to make the homopolymer distribution more uniform. Since low molecular weight homopolymers have a high entropy of mixing, they favor a broader distribution which increase the area per junction as observed in the experiment. On the contrary, homopolymers of higher molecular weights have a tendency to localize near the center of the lamellar. As we will see below, these theoretical expectations are in accord with our experimental findings.

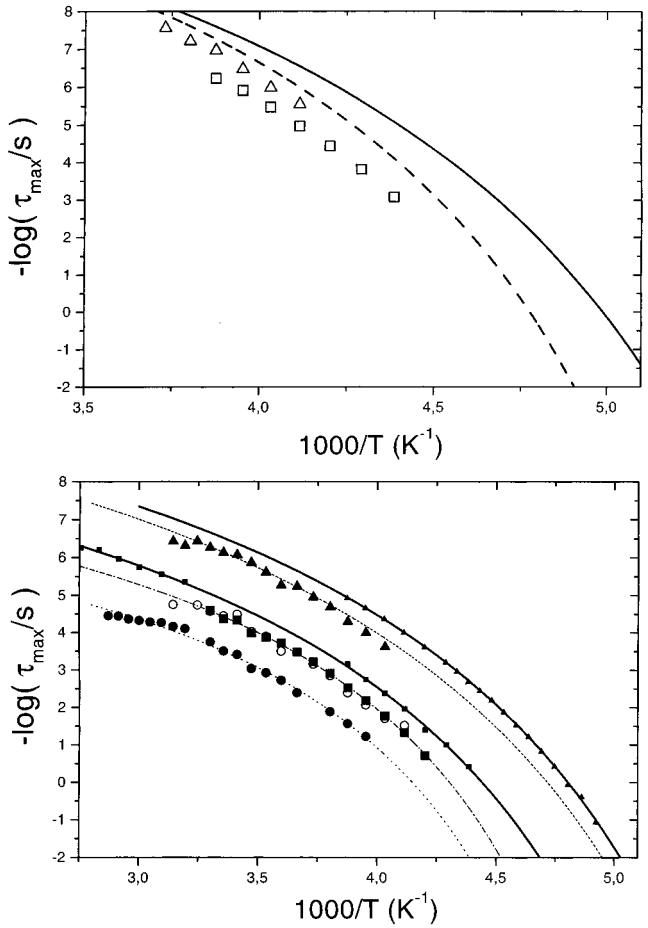

Figure 3. (a, top) Arrhenius plot of the relaxation times corresponding to the single segmental mode in the blends SI-22500/PI-1200 (triangles) and SI-22500/PI-4900 (squares). The corresponding modes in the PI-1200 and PI-4900 homopolymers are also shown with solid and dashed lines, respectively, which are fits to the VFT equation (see text). (b, bottom) Arrhenius plot of the relaxation times corresponding to the normal modes in the same blends as in (a). The PI-1200 homopolymer normal mode in the SI-22500/PI-1200 blend is shown with filled triangles. The block relaxation in the SI-22500 is shown with filled circles. The block relaxation in the SI-22500/PI-1200 blend is shown with open circles, and the single normal mode in the SI-22500/PI-4900 blend is shown with filled squares. Solid lines give the VFT fits to the PI-1200 (small triangles) and PI-4900 longest normal mode (small squares). All lines are fits to the VFT equation (see text).

Dynamics. An example of the dynamic signature of the homopolymer addition to the SI microdomains is shown in Figure 2. The dielectric loss spectra are shown for the SI-22500/PI-1200 (80/20) blend at some temperatures in the range 238−258 K. There are clearly three peaks corresponding to the fast (single) segmental mode, to the PI homopolymer normal mode, and to the "slow" PI block relaxation. The data have been normalized to the segmental peak and reveal that with decreasing temperature the slow normal modes shift toward the segmental peak. This observation, that is, the different shift factors of the segmental and normal modes in type A homopolymers, has been discussed in terms of the breakdown of the Rouse model in polymer melts.[16]

We have followed the dynamics of the blends as a function of temperature, and in Figure 3a we compare the segmental dynamics in two blends—SI-22500/PI-1200 and SI-22500/PI-4900—with the bulk homopolymer and diblock copolymer dynamics. In both cases there is a single segmental mode in the blends which is slightly

slower than the homopolymer segmental dynamics. This might originate from PI segments at the SI interface. We can obtain an estimate of the interfacial thickness from[17]

$$\Delta \approx \Delta_\infty \left[1 + \frac{1.34}{(\chi N)^{1/3}}\right] \tag{7}$$

where Δ_∞ ($= 2a/(6\chi)^{1/2}$, assuming $a_{PS} = a_{PI} = a$ for the statistical segment length) is the interfacial thickness in the limit $\chi N \rightarrow \infty$.[18] For the SI-22500 diblock ($N =$ 266, $c = 0.079$, $a = 0.68$ nm) we obtain an interfacial thickness of 3 nm. This value should be compared with the long spacing of 18.5 nm. We conclude that a significant fraction (about 20%) of the PI chains are located within the interface.

The lines in Figure 3a are fits to the Vogel−Fulcher−Tammann (VFT) equation:

$$\log \tau = \log \tau_0 + \frac{B}{T - T_0} \tag{8}$$

where $\log \tau_0$ is the limiting value at high temperatures, B is the apparent activation energy, and T_0 is the "ideal" glass transition temperature. These parameters assume the values 13.9, 664 K, and 153 K for PI-1200 and 13.9, 617 K, and 165 K for PI-4900. The rest of the segmental mode dynamics will be discussed later with respect to the normal mode dynamics in the blends.

In Figure 3b we plot the normal mode dynamics in the same blends (SI-22500/PI-1200 and SI-22500/PI-4900). Again solid lines correspond to the PI-1200 and PI-4900 homopolymer normal modes with VFT parameters: 10.8, 646 K, 149 K and 9.4, 620 K, 158 K, respectively. The normal mode of PI-1200 in the blend (with VFT parameters: 10.7, 685 K, 150 K) slows down but to a lesser extent than the segmental mode, as discussed previously with respect to Figure 2 and ref 16. On the other hand, the block relaxation in the same blend speeds up as compared to the PI block relaxation in the SI-22500 (with VFT parameters: 7.3, 443 K, 180 K) nearly by 1 decade. In the SI-22500/PI-4900 blend there is a single chain relaxation (VFT parameters: 8.3, 480 K, 175 K) which again is faster than the PI chain relaxation in the SI-22500.

In parallel with the dynamics we discuss the intensity of the processes in Figure 4. The dielectric strength of the normal mode process is related to the end-to-end distance by[8,9]

$$\Delta\epsilon = \frac{4\pi\varphi_{PI} N_A \mu^2}{3k_B T} \frac{\langle r^2 \rangle}{M_{PI}} \tag{9}$$

where φ_{PI} is the PI concentration in the blends, N_A is Avogadro's number, μ is the dipole moment per contour length, and M_{PI} is the molecular weight of the PI chain. In Figure 4, we plot the product $T\Delta\epsilon$ for the homopolymer and block relaxations in the blend SI-22500/PI-1200 and in the bulk SI-22500 as a function of inverse temperature. First, for the homopolymer relaxation, we find that a fraction of the intensity is missing. This can be explained by the fact that short PI chains can act as a solvent and therefore can participate in both phases as well as within the interface. This explains also the plasticization of the PS glass transition from DSC (Table 3). For the block relaxation, on the other hand, we find a distinctly different behavior. The PI block intensity

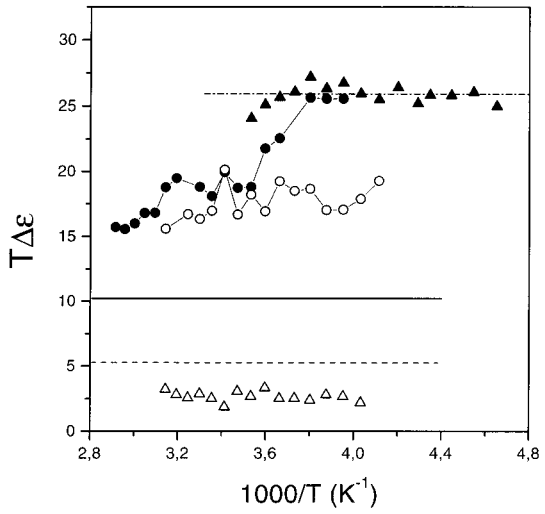

Figure 4. Relaxation strength ($T\Delta\epsilon$) plotted versus inverse temperature for the different processes in the SI-22500/PI-1200 blend. The values for the normal mode of the PI-1200 homopolymer in the bulk are also shown (filled triangles) and are compared with the same process in the blend (open triangles). Likewise, the PI block relaxation in the SI-22500 diblock (filled circles) is compared with the same relaxation in the blend (open circles). Dash−dotted, solid, and dashed lines give the theoretical predictions for the relaxation strength of the PI-1200 normal mode in the bulk, the PI block, and the PI-1200 homopolymer in the blend.

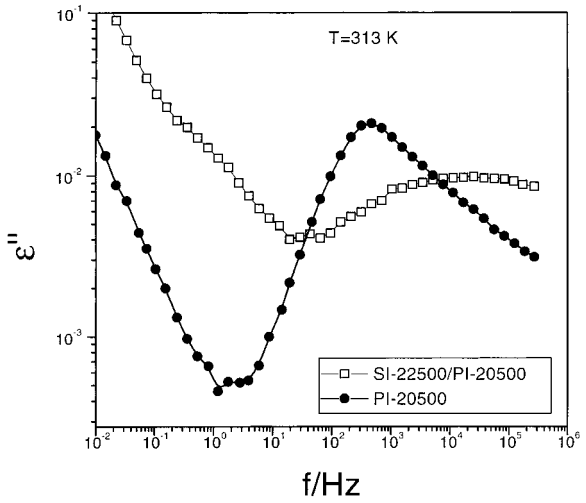

Figure 5. Comparison of the dielectric loss spectra of SI-22500/PI-20500 blend with the PI-20500 homopolymer at 313 K. Notice that the single chain mode in the blend shifts to higher frequencies (i.e., becomes faster) as compared to the same mode in the PI homopolymer.

in the pure diblock SI-22500 exhibits a strong T dependence. Such a dependence can originate from the increasing stretching of the PI chains with decreasing T. Addition of the homopolymer clearly lessens block stretching as indicated by the weaker T dependence. However, the block intensity is still higher than the theoretical expectation for a purely Gaussian chain of the same length ($\langle r^2 \rangle = Na^2$, where $a = 0.68$ nm is the statistical segment length for PI), meaning that despite the PI homopolymer addition the PI blocks in the blend are still stretched.

In going into longer PI chains, we find a very different dynamic behavior. Figure 5 compares the dielectric loss spectra of the SI-22500/PI-20500 (80/20) blend with the PI-20500 homopolymer at 313 K. In contrast to the case from the lower molecular weights, the single chain

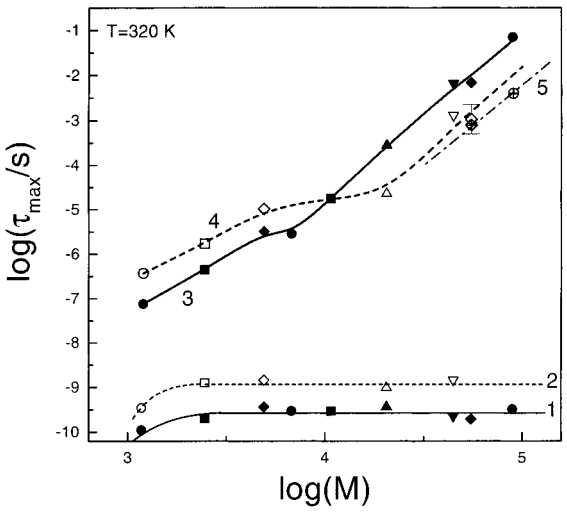

Figure 6. Molecular weight dependence of the segmental and longest normal modes in the SI-22500/PI (80/20) blends at 320 K. Five data sets are shown: set 1, segmental modes of PI homopolymers in the bulk; set 2 (short dash line), segmental modes of the same PI's in blends with SI-22500; set 3 (the solid line is a guide to the eye), longest normal mode of PI homopolymers in the bulk; set 4 (dashed line), chain relaxation of the same PI's in blends with SI-22500; set 5 (dash−dotted line), longest normal mode for the PI-55000 and PI-90000 in their blends with PI-10800. The different dynamic regimes and data sets are discussed in the text.

relaxation in the blend now speeds up. In fact, for all $M_{PI} > M_e$, where M_e (=5000) is the entanglement molecular weight for PI, the homopolymer normal mode speeds up. The results for the segmental and homopolymer normal mode dynamics in the SI-22500/PI blends are summarized in Figure 6 at 320 K. Five data sets are shown indicated with numbers. Data set 1 corresponds to the segmental mode of PI homopolymers in the bulk and data set 2 to the same mode in the SI-22500/PI blends. The dynamics of the segmental modes in the two cases have an identical dependence on M_{PI}. With decreasing M_{PI} there is a speedup of the segmental dynamics that originates from the depression of the T_g^{PI} due to chain-end effects also seen in the calorimetric study (Table 3). Data set 3 gives the longest normal mode of PI homopolymers in the bulk. The different slopes below and above M_e can be accounted for by the Rouse ($M < M_e$) and reptation ($M > M_e$) models, respectively. The steeper slope in the latter case found in the experiments (compared with the 3.0 slope predicted by the pure reptation theory[19]) has been discussed in terms of contour length fluctuations and tube reorganization models.[19] Data set 4 corresponds to the homopolymer longer normal mode within the PI domain of the diblock copolymer. The molecular weight dependence of this mode can be discussed in terms of three regimes. For $M < M_e$ the slowdown of the PI relaxation in the blends can be accounted completely by the slowdown of the segmental mode, i.e., local friction effects. For $M \approx M_e$ the single normal mode in the blends originating from both the block and the homopolymer relaxation exhibit a weak dependence on the molecular weight. Finally, for $M > M_e$ the homopolymer chain relaxation in the blends becomes *faster* than the same mode in the bulk homopolymer. In the same figure, data set 5 gives the longest normal mode relaxation of the minority component in binary blends of PI-10800/PI-55000 (80/20) and PI-10800/ PI-90000 (80/20) and will be discussed below in detail.

In the next section we will account for the different dynamic responses of the PI homopolymer and block in the SI/I blends, at least in a qualitative way. First we discuss the case $M < M_e$. For such short chains the homopolymer acts practically as a solvent, and in the length scale of the homopolymer, the slowing down of the normal mode comes entirely from the local friction with a Rouse time:

$$\tau_R = \tau_0 N^2 \tag{10}$$

where $\tau_0 = \zeta_0 a^2/3\pi^2 k_B T$ is the monomer time and ζ_0 is the monomeric friction coefficient. Therefore, a simple correction for the segmental times (through ζ_0) will bring the homopolymer normal mode dynamics in the blends in coincidence with the same times in the bulk homopolymers (Figure 6). On the other hand, on the length scale of the block relaxation we found (Figure 3b) that the PI block speeds up. The PI block with a molecular weight of 10 100 is (lightly) entangled. However, due to the localization of the junction point at the interface, the blocks cannot reptate. Instead, the relevant mechanism for the block relaxation is arm retraction similar to a star polymer. The latter mechanism has intensity[20]

$$I \approx N(\chi N)^{1/3} \tag{11}$$

and dynamics

$$\tau \approx \left(\frac{\zeta_0 a^2}{3\pi^2 k_B T}\right)\frac{N^3}{N_e}\exp\left[\frac{N}{2N_e}\right] \tag{12}$$

Blending the SI diblock with short PI homopolymers results in a dilution of entanglements ($N_{e,eff} > N_e$) at the block length scale, and this can account for the observed speedup through eq 12.

When $M > M_e$, on the homopolymer length scale, Figure 6 indicates a speedup of the homopolymer normal mode. In this regime the relevant homopolymer dynamics are described by the reptation theory as

$$\tau_{rep} = \left(\frac{\zeta_0 a^2}{3\pi^2 k_B T}\right)\frac{N^3}{N_e} \tag{13}$$

In the SI/I blend N_e in eq 13 should be replaced by an effective $N_{e,eff}$, which is now higher than the pure homopolymer case since blending of the long homopolymer with the shorter PI blocks of the SI copolymer results in a dilution of the entanglements. A more quantitative comparison, however, would require a 10-fold increase of the entanglement molecular weight for a speedup of the homopolymer normal mode by 1 decade. This would practically mean that our PI homopolymer chains in the blends are barely entangled which is not very realistic. Therefore, the use of the reptation theory with a modified N_e ($N_{e,eff}$) only qualitatively describes the experimental findings in Figure 6. In the intermediate range ($M \approx M_e$) the two effects for the extreme cases produce nearly a flat line (i.e., molecular weight independent times). This range can be viewed as a transition regime between the low molecular weights (where local friction effects dominate) and high molecular weights (reptation with entanglement dilution).

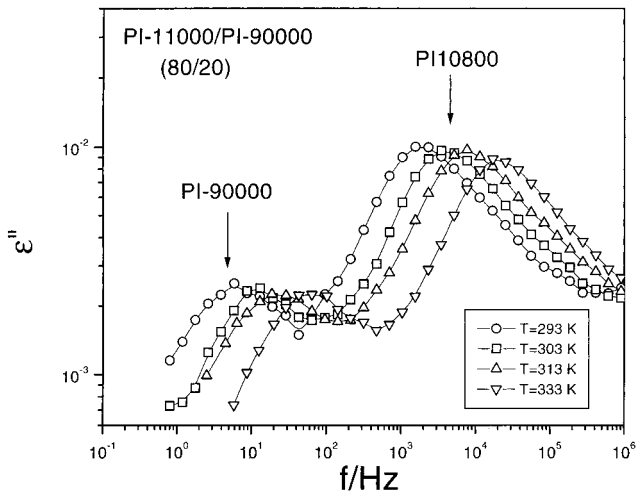

Figure 7. Normal mode dynamics in the blend PI-10800/PI-90000 (80/20) at different temperatures as indicated. The slow and fast modes correspond to the PI-90000 and PI-10800 normal modes in the blend.

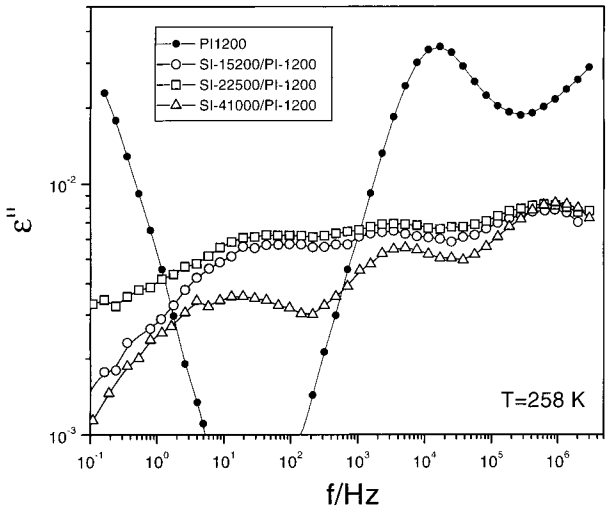

Figure 8. Dielectric loss for the blends of PI-1200 in three symmetric diblock copolymers: SI-15200, SI-22500, and SI-41000 at 258 K. The spectrum of the PI-1200 homopolymer in the bulk is also shown at the same temperature.

Another effect that can influence the homopolymer chain dynamics within the SI microdomains is the possible localization (of the homopolymer) near the center of the PI domain. As we discussed earlier with respect to the structure, the longer the PI the lower the entropic effect and the more localized is the homopolymer near the lamellar center. Such an effect would tend to increase the relaxation times toward the bulk homopolymer values. To check this possibility, we have prepared blends of a PI with molecular weight of 10 800 (i.e., comparable to the PI in the SI-22500 diblock) with two PI's with molecular weights of 5.5×10^4 and 9.0×10^4. Some typical dielectric loss spectra for the PI-10800/PI-90000 (80/20) blend are shown in Figure 7 at some temperatures. The figure shows individual normal mode spectra corresponding to the PI-90000 and PI-10800 chains in the blend. At higher frequencies there is a faster mode corresponding to the single segmental mode in the blend. The relaxation times corresponding to the PI-90000 and PI-55000 longest normal modes in the blends are plotted in Figure 6 (with the dash−dotted line) and give the fastest possible relaxation of the PI homopolymers, i.e., dynamics with the effect of dilution of entanglements but without the effect of localization. The difference between the two sets of data is small, but it signifies that the speedup of the homopolymer dynamics in the blends (for $M > M_e$) is a composite effect originating mainly from the dilution of entanglements (speedup) and to a smaller extent by the localization of PI near the center of the domain (slowdown). Clearly the effect of homopolymer localization on the dynamics is only expected for very high molecular weights. Macrophase separation, however, precludes such an investigation. For short molecular weights, the entropic effects that favor a broader distribution dominate. These theoretical expectations are in good agreement with the homopolymer dynamics shown in Figure 6.

In a second study the same homopolymer (PI-1200) was inserted in different nearly symmetric SI diblock copolymers (SI-15200, SI-22500, and SI-41000) with increasing degree of segregation (i.e., from χN of about 16−28). The purpose of this study is to explore the effect of block incompatibility on the homopolymer relaxation. Figure 8 gives the dielectric loss spectra of the three blends and of the PI-1200 homopolymer at 258 K. In

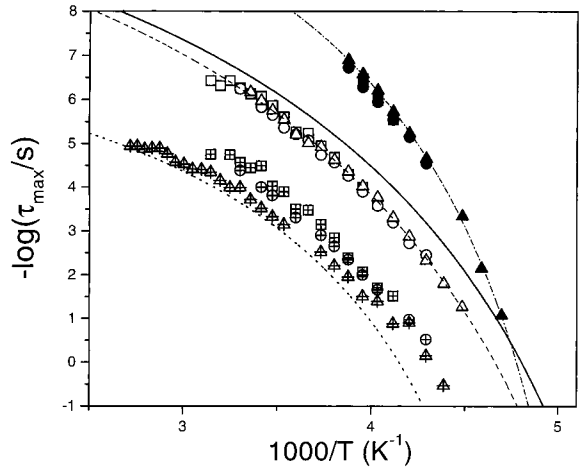

Figure 9. Relaxation map for the dynamics in blends of PI-1200 with SI-15200 (circles), SI-22500 (squares), and SI-41000 (triangles). The segmental (filled symbols), the PI-1200 longest normal mode (open symbols), and the block relaxations are shown. The dash−dotted, dashed, and dotted lines are VFT fits to the segmental, homopolymer longest normal mode in the blend, and the PI block relaxation in the SI-22500, respectively. The solid line is the result of the VFT fit to the PI-1200 longest normal mode in the bulk.

accord with the first study, there is a single segmental mode in all blends relaxing with the same rate and two slower modes corresponding to the homopolymer chain and block relaxations. The dynamics in the three blends are compared in Figure 9 in the usual Arrhenius representation. The segmental mode in the three blends can be described by the VFT equation with parameters $\log \tau_0$, B, and T_0: 12.4, 485 K, and 170 K, respectively. Similarly, the homopolymer chains relax with the same rate in all blends with VFT parameters: 10.9, 720 K, and 149 K. This relaxation is again slower than the pure homopolymer longest normal mode by about 1 order of magnitude, reflecting purely local friction effects through the prefactor in eq 10. On the other hand, the intensity of the homopolymer chain relaxation in the blends was found to increase with increasing block segregation approaching the theoretical value in the SI-41000/PI-1200 blend. In the SI-15200 and SI-41000 diblocks the average area per junction on the PS−PI interface

amounts to 36 and 50 nm^2, respectively. In their blends with PI-1200, the corresponding values are 44 and 61 nm^2, indicating a similar increase of lateral expansion (about 20%). On the basis of this structural information, we conclude that increasing the thermodynamic field (i.e., χN) in the block copolymers does not alter the homopolymer profile but only the number of relaxing homopolymer units through the incorporation of homopolymer chains from the interface and from the PS to the PI domain. In this respect it would be interesting to investigate also homopolymers of higher molecular weights. Last, on the block length scale, the speedup can be understood by the arm retraction mechanism with a diluted effective entanglement spacing as described by eq 12.

V. Conclusion

We have studied the dynamics in block copolymer/homopolymer blends as a function of the thermodynamic field for a given homopolymer and as a function of homopolymer length for a given diblock copolymer. The thermodynamic field of microphase separated block copolymers imposes structural changes which reflect nicely on the homopolymer and block dynamics. The structure investigation revealed that for long homopolymers there is tendency for localization within the center of the domain. This structural picture alters the topological constraints and has many consequences on the homopolymer and block dynamics. As a result, the homopolymer dynamics within a diblock copolymer can be discussed in terms of three regimes ($M < M_e$, $M \approx M_e$, $M > M_e$). For $M < M_e$, local friction effects account for the modification of the homopolymer dynamics. For $M > M_e$, the modification has two origins with opposing trends: reptation and confinement effects. Reptation accounts only qualitatively for the modification since an exact comparison would require a large increase of M_e. On the other hand, for the block dynamics the arm-retraction mechanism qualitative accounts for the experimental findings. Overall, we find that the thermodynamic nature of the confinement in block copolymer/homopolymer blends is responsible for the alteration of the structure and the associated dynamics.

Acknowledgment. We thank Prof. A. N. Semenov for fruitful discussions.

References and Notes

(1) Jackson, C. L.; Mckenna, G. B. *J. Chem. Phys.* **1990**, *93*, 9002.
(2) Jackson, C. L.; Mckenna, G. B. *J. Non-Cryst. Solids* **1991**, *131−133*, 221.
(3) Hofer, K.; Mayer, E.; Johari, G. P. *J. Phys. Chem.* **1991**, *95*, 7100.
(4) Petychakis, L.; Floudas, G.; Fleischer, G. *Europhys. Lett.* **1997**, *40*, 685.
(5) Leibler, L. *Macromolecules* **1980**, *13*, 1602.
(6) See for example: Floudas, G.; Ulrich, R.; Wiesner, U. *J. Chem. Phys.* **1999**, *110*, 652 and references therein.
(7) Floudas, G.; Hadjichristidis, N.; Stamm, M.; Likhtman, A. E.; Semenov, A. N. *J. Chem. Phys.* **1997**, *106*, 3318.
(8) (a) Stockmayer, W. H. *Pure Appl. Chem.* **1967**, *15*, 539. (b) Bauer, M. E.; Stockmayer, W. H. *J. Chem. Phys.* **1965**, *43*, 4319. (c) Adachi, K.; Kotaka, T. *Macromolecules* **1985**, *18*, 466. (d) Boese, D.; Kremer, F. *Macromoelcules* **1990**, *23*, 829. (e) Yao, M.-L.; Watanabe, H.; Adachi, K.; Kotaka, T. *Macromolecules* **1991**, *24*, 2955.
(9) (a) Floudas, G.; Hadjichristidis, N.; Iatrou, H.; Pakula, T. *Macromolecules* **1996**, *29*, 3139. (b) Floudas, G.; Alig, I.; Avgeropoulos, A.; Hadjichristidis, N. *J. Non-Cryst. Solids* **1998**, *235−237*, 485. (c) Alig, I.; Floudas, G.; Avgeropoulos, A.; Hadjichristidis, N. *Macromolecules* **1997**, *30*, 5004. (d) Floudas, G.; Paraskeva, S.; Hadjichristidis, N.; Fytas, G.; Chu, B.; Semenov, A. N. *J. Chem. Phys.* **1997**, *107*, 5502.
(10) Floudas, G. Manuscript in preparation.
(11) Mori, K.; Okawara, A.; Hashimoto, T. *J. Chem. Phys.* **1996**, *104*, 7765.
(12) Semenov, A. N. *Sov. Phys. JETP* **1985**, *61*, 733.
(13) Melenkevitz, J.; Muthukumar, M. *Macromolecules* **1991**, *24*, 4194.
(14) Winey, K. I.; Thomas, E. L.; Fetters, L. J. *Macromolecules* **1991**, *24*, 6182.
(15) Matsen, M. W. *Macromolecules* **1995**, *28*, 5765.
(16) Plazek, D. J.; Schlosser, E.; Schonhals, A.; Ngai, K. L. *J. Chem. Phys.* **1992**, *25*, 4915. Plazek, D. J.; Bero, C. A.; Neumeister, S.; Floudas, G.; Fytas, G.; Ngai, K. L. *Colloid Polym. Sci.* **1994**, *272*, 1430. Ngai, K. L.; Plazek, D. J. *Rubber Chem. Technol. Rubber Rev.* **1995**, *68*, 376. Nicolai, T.; Floudas, G. *Macromolecules* **1998**, *31*, 2578. Floudas, G.; Reisinger, T. *J. Chem. Phys.* **1999**, *111*, 5201. Floudas, G.; Gravalides, C.; Reisinger, T.; Wegner, G. *J. Chem. Phys.*, in press.
(17) Semenov, A. N. *Macromolecules* **1993**, *26*, 6617.
(18) Helfand, E.; Tagami, Y. *J. Chem. Phys.* **1971**, *56*, 3592.
(19) Doi, M.; Edwards, S. F. *The Theory of Polymer Dynamics*; Oxford University Press: Oxford, 1986.
(20) Semenov, A. N. Personal communication.

MA990524N